Is collisionless heating in capacitively coupled plasmas really collisionless?

2015 Plasma Sources Sci. Technol. 24 044002

(http://iopscience.iop.org/0963-0252/24/4/044002)

IOP Publishing Plasma Sources Science and Technology

Plasma Sources Sci. Technol. **24** (2015) 044002 (10pp) doi:10.1088/0963-0252/24/4/044002

Is collisionless heating in capacitively coupled plasmas really collisionless?

T Lafleur[1,2] **and P Chabert**[1]

[1] Laboratoire de Physique des Plasmas, CNRS, Sorbonne Universités, UPMC Univ Paris 06, University Paris-Sud, Ecole Polytechnique, 91128 Palaiseau, France
[2] ONERA-The French Aerospace Lab, 91120 Palaiseau, France

E-mail: trevor.lafleur@lpp.polytechnique.fr

Received 3 March 2015, revised 29 April 2015
Accepted for publication 18 May 2015
Published 19 June 2015

Abstract

By performing a combination of test-particle and particle-in-cell simulations, we investigate electron heating in single frequency capacitively coupled plasmas (CCPs). In agreement with previous theoretical considerations highlighted in Kaganovich *et al* (1996 *Appl. Phys. Lett.* **69** 3818), we show that the level of true collisionless/stochastic heating in typical CCPs is significantly smaller than that due to collisional interactions; even at very low pressures and wide gap lengths. Fundamentally electron heating is a collisional phenomenon whereby particle collisions provide the vital phase randomization and stochastization mechanism needed to generate both a local (or ohmic) heating component, and a non-local (or hybrid) heating component.

Keywords: collisionless heating, stochastic heating, capacitively coupled plasma, CCP, particle-in-cell

(Some figures may appear in colour only in the online journal)

1. Introduction

Since some of the earliest experimental measurements [1, 2] of rf capacitively coupled plasmas (CCPs), it has been known that ohmic heating alone cannot explain the observed power absorption at low pressures. Consequently, the concept of collisionless or stochastic electron heating has become well established in the rf plasma community [3–5]. Here electrons are generally viewed as being heated by interactions with the oscillating sheaths at each rf electrode, which is in contrast to ohmic heating, where collisions between electrons and heavy particles provide the necessary phase randomization (between the electron motion and the rf electric field) to produce a net power absorption. Collisionless heating has also become associated with the appearance of bi-Maxwellian electron distribution functions [2, 3, 6], which are typically characterized by a low-temperature population of electrons at energies below about 5 eV, and a higher temperature population above 5 eV that maintains the discharge ionization balance. Since the majority of electrons form part of the low-temperature population, the average electron energy is very low [2] (contrary to theoretical expectations based on pressure-length arguments [3, 4]), and this is usually correlated with an increased plasma density.

Electron heating, and particularly collisionless heating, continues to be a widely studied phenomenon, with many experimental [1, 2, 7–10], numerical [6, 11–16], and theoretical contributions [17–22]. Since it is impossible to directly measure collisionless power absorption, experimental work has typically focused on indirect evidence, such as estimates obtained by subtracting off ohmic heating contributions from the total measured power [1, 2, 7], measurements of bi-Maxwellian electron distribution functions [2, 7], or measurements of the spatio-temporal excitation rate using optical emission spectroscopy [8–10]. More detailed fundamental physics studies have been performed using particle-in-cell (PIC) simulations, which have proven to be indispensible tools in aiding our understanding of the electron heating process in CCPs. This numerical work has demonstrated the formation of electron beams correlated with the expanding rf sheaths [11, 13], as well as the subsequent enhancement and modulation of the ionization rate [11, 13], and the strong contribution that the electric field in the near-sheath region has on the power absorption [6, 11, 15, 16]. Other PIC simulations have taken a

more quantitative approach by subtracting off the collisional heating component (often estimated using a quasi-analytical model) from the total power [16, 23], or by analysing the power absorption using a moment method [14, 15, 24] (typically based on the electron mechanical energy conservation equation), to identify and determine the importance of specific electron heating components. These simulations have shown that electron heating can be decomposed into two dominant parts: a local collisional (or ohmic) part, and a part related to the electron pressure gradient (pressure heating). This pressure heating component has recently been shown [22] to correspond to that which current theoretical collisionless heating models predict.

While it is tempting to directly associate pressure heating with true collisionless heating, this has so far been difficult to definitely conclude from simulations alone, and a close scrutiny of the most widely used theoretical collisionless heating models [18, 20, 22] identifies a number of inconsistent and unsatisfactory assumptions present. For example, both the hardwall [17, 18, 21] and kinetic-fluid models [20] treat only a semi-infinite plasma, and do not follow particle trajectories or self-consistently determine the electron distribution function. In addition, the sheath edge is treated as a perfectly reflecting boundary in the hardwall model, while assumptions on the form of the electron heat flux and spatial temperature distribution are needed in the kinetic-fluid model. As a result, these models cannot be claimed to truly predict collisionless electron heating. It is thus fair to say that a number of fundamental questions on the nature of electron heating have not yet been answered. Or, in the context of the above discussion, we can state this more specifically: is the non-ohmic heating component in CCPs really due to collisionless heating?

An answer to the above question is of particular importance, because the terms 'collisionless' or 'stochastic' heating are widespread within the literature, and have become synonymous with any electron heating component different from ohmic. Thus one is given the impression that collisionless heating is essentially guaranteed in all low pressure CCPs. Indeed all of the theoretical electron heating models based on the Fermi-acceleration/hardwall mechanism [17, 18, 21] predict electron heating in the absence of any particle collisions. In addition, these models seem to agree well with PIC simulation results [16, 23, 25]. However, more rigorous theoretical work [26, 27] based on non-local kinetic theory and the energy diffusion coefficient [28], has shown that although stochastic heating is an important mechanism in low pressure inductively coupled plasmas, in bounded CCPs the electron motion is regular, stochastic heating is small, and the Fermi-acceleration mechanism is not significant. In this case the non-ohmic electron heating component is still collisional, but non-local; phase randomization occurs due to collisions that take place at a different location to the electron energy gain from the rf sheaths. More recently, by tracking individual particles, PIC simulations [24] have suggested that electron heating requires multiple electron collisions with the same sheath during an rf period; a process that relies strongly on electron-neutral collisions.

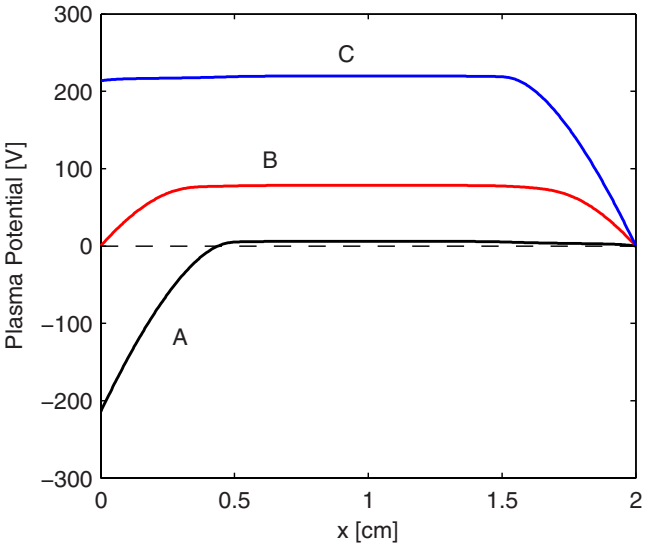

Figure 1. Example of the spatial profile of the plasma potential used in the TP simulations at three different rf phases: when the right-hand side sheath has fully expanded (A), when the sheaths are symmetric (B), and when the left-hand side sheath has fully expanded (C). The plasma potential has been taken from current-driven full PIC simulations run at 100 mTorr, a gap length of 2 cm, and an rf current density amplitude of 25.6 Am^{-2}.

Thus a conundrum exists: is non-ohmic electron heating really collisionless/stochastic as Fermi-acceleration/hardwall models suggest, or are collisional interactions required as predicted by non-local kinetic theory? That is, is 'collisionless' heating, really collisionless? The aim of this paper is to specifically investigate this question, and at the same time stimulate further discussion on the important topic of electron heating.

2. Description of simulation

To investigate electron heating we make use of a 1D3V kinetic particle simulation (which we will call a test-particle (TP) simulation), where electrons are treated as non-interacting test particles exposed to a spatio-temporally varying potential located between two parallel rf electrodes. This potential is obtained from full PIC simulations (an example of which is shown in figure 1), and as a result, ion trajectories, as well as Poisson's equation, do not need to be solved in the TP simulations. The electrons are moved using the standard leap-frog scheme, and any electrons lost to the electrodes are replaced by new electrons whose positions are determined randomly from the spatial distribution of the ionization rate profile obtained from the full PIC simulations. The velocity of these new electrons is either chosen from a non-drifting Maxwellian distribution with a given temperature, or from a drifting Maxwellian with a spatio-temporally varying drift velocity and electron temperature:

$$f(x, v, \theta) \propto \exp\left[-\frac{m(v-u)^2}{2k_{\mathrm{B}}T_e}\right] \tag{1}$$

Here m is the electron mass, v is the electron velocity, $u = u(x, \theta)$ and $T_e = T_e(x, \theta)$ are the spatio-temporally varying

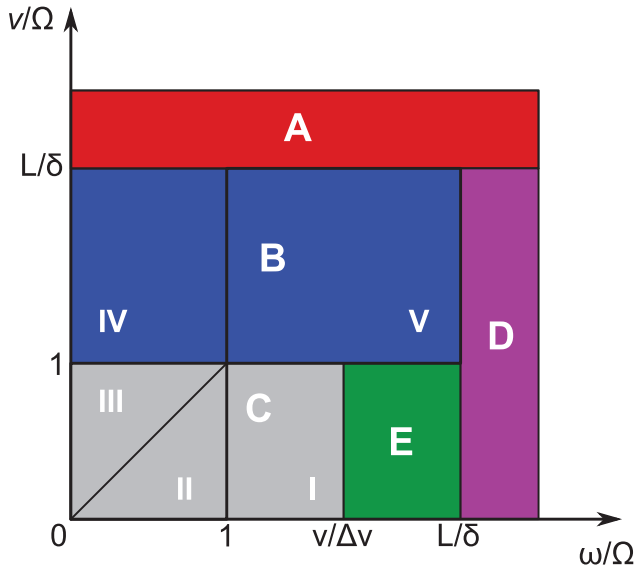

Figure 2. Schematic diagram of the different dominant electron heating regimes with: (A) ohmic heating, (B IV, and V) hybrid heating with frequent collisions, (C I, II, and III) hybrid heating with rare collisions, (D) high-frequency limit, (E) true collisionless heating. This figure has been modified from [26].

drift velocity and electron temperature, k_B is Boltzmann's constant, and θ is the rf phase. The drift velocity and electron temperature are obtained from the full PIC simulations by taking the relevant electron velocity moments weighted to the PIC grid. In principle a more accurate method for loading the new electrons in phase space is to choose them from the exact velocity distributions at the new particle position and rf phase from the full PIC. However, in order to obtain sufficient particle statistics, this method is very computationally expensive, and so the approximate method described above is used.

The full PIC simulations mentioned above include both narrow-gap (2 cm) simulations, as well as wide-gap (6.7 cm) simulations, which are based on the well-known argon CCP experiments of [2, 7]. The narrow-gap simulations have been previously described and benchmarked in [15], and are current-driven with an amplitude of 25.6 Am^{-2}, pressures between 70–1000 mTorr, 400 grid points, a few hundred thousand particles, and a time step of $\Delta t \sim 6 \times 10^{-12}$ s. The wide-gap simulations are run for pressures between 3–30 mTorr, an amplitude of 10 Am^{-2}, and a time step twice as large (because of the lower plasma density [29, 30]). For the spatio-temporal potential, ionization rate, drift velocity, and electron temperature, the results are averaged (at the correct rf phase) over a few hundred rf periods to reduce statistical noise levels. In the TP simulations the electrons are moved using the same time step as that in the full PIC, but fewer particles (around 10 000) are needed since Poisson's equation is not solved. The TP simulations use the same Monte Carlo collision algorithm as the PIC (which includes elastic and inelastic collisions), but only the energy loss is modelled during ionization reactions; new electrons are not added to the simulation. In the results to follow, true collisionless heating is studied by separately turning on and off electron-neutral collisions in these simulations.

The above TP simulation scheme is somewhat similar to that used in [31], except that we use pre-calculated electric fields obtained from a full PIC simulation instead of a hybrid fluid model. We also follow the test electrons for 1000–2000 rf periods to allow the distribution to evolve/relax in the applied fields.

3. Electron heating regimes

The importance of heavy particle collisions on electron heating has been explicitly studied by Kaganovich *et al* [26], where a classification scheme was introduced to identify different heating regimes possible. This scheme was constructed by considering three primary frequencies of interest in low pressure plasmas: the angular excitation frequency of the rf fields, $\omega = 2\pi f$, the electron collision frequency, $\nu = n_g \sigma v$, and the electron bounce frequency between opposite walls of the discharge, $\Omega = v_x/2L$. Here f is the applied rf frequency, n_g is the neutral gas density, σ is the cross-section for electron-neutral collisions, v is the electron speed, v_x is the electron velocity along the discharge length, and L is the discharge length. Different dominant heating scenarios are then determined based on the ratios, ν/Ω and ω/Ω. Using a representative electron velocity given by the thermal velocity, $v_t = \sqrt{qT_e/m}$ (where q and m are the electron charge and mass respectively, and T_e is the electron temperature), and assuming $v \sim v_x \sim v_t$, these ratios become

$$\frac{\nu}{\Omega} = 2n_g L\sigma = \frac{2L}{\lambda} = \frac{2}{\mathrm{Kn}} \tag{2}$$

$$\frac{\omega}{\Omega} = \frac{4\pi f L}{v_t} \tag{3}$$

Here $\lambda = 1/n_g\sigma$ is an electron mean free path, and thus we see that equation (2) is related to a Knudsen number ($\mathrm{Kn} = \lambda/L$). According to the heating scheme in [26], there are four main electron heating regimes present in CCPs, which we have illustrated schematically in figure 2. For $\nu/\Omega \gg 1$ (region A in figure 2) collisions are very frequent, and ohmic heating is the main power deposition mechanism. For $\nu/\Omega > 1$ (region B in figure 2) hybrid heating dominates, and collisions play an important non-local role; the location of electron energy gain by the sheath electric fields is different to the location where phase randomization by heavy particle collisions occurs. For $\nu/\Omega < 1$ and $\omega/\Omega < v/\Delta v$ (region C I in figure 2), collisions are very rare, but are still needed to generate a net heating. Here Δv is the electron velocity gain after a collision with an oscillating rf sheath. Finally, for $\nu/\Omega < 1$ and $\omega/\Omega > v/\Delta v$, a regime (region E in figure 2) exists in which true collisionless/stochastic heating is dominant.

Despite the introduction of these different heating regimes, a distinction is almost never made in the literature, and the terms collisionless or stochastic heating are used for any electron heating component different from ohmic heating [3, 4]. Our interest here is to investigate some of these heating

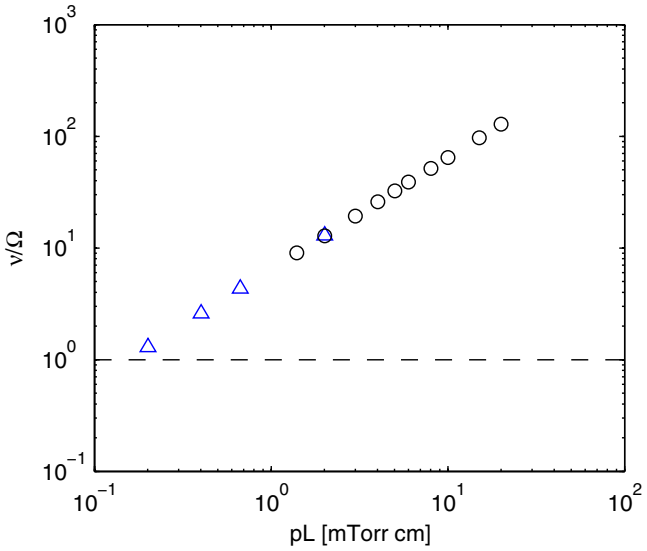

Figure 3. Ratio of the collision frequency to the bounce frequency, ν/Ω, as a function of pressure multiplied by the discharge gap length. The open triangles show the ratio for a gap length of 6.7 cm, while the open circles show the ratio for a gap length of 2 cm.

regimes, and to confirm the results of Kaganovich *et al* [26] that the level of true stochasticity present in CCPs at conditions typical of most industrial or research reactors is very low. In this regard, as mentioned in section 2, we investigate pressures between 3–1000 mTorr, and gap lengths of 2 cm and 6.7 cm. While stochastic heating is not expected at the higher pressures, we have included them for completeness. This also allows a useful comparison with the intermediate pressure range, which is the one most often encountered experimentally.

For the chosen pressure and length conditions (and using a representative electron temperature of 3 eV and a collision cross-section of $\sigma \approx 1 \times 10^{-19}$ m^2 for argon taken from [32]), we find $\omega/\Omega = 4.7$ and 15.7 respectively, while ν/Ω varies between about 1 and 100, as shown in figure 3. The lower pressure range for these tests corresponds to the case where $\lambda \sim L$; i.e. an electron will on average traverse the gap between the electrodes before having a collision. This can thus be argued as a 'collisionless' regime, and so stochastic heating would be expected to be relevant here.

Based on the classification scheme discussed above, we see that the chosen operating conditions span the ohmic and hybrid heating regimes. In order to access the true collisionless/stochastic heating regime (region E in figure 2) it is necessary for lower pressures to be used. However, both experimentally [7] and numerically it is difficult to sustain a plasma, and so one can argue that this regime is not actually encountered in most practical systems, and indeed would correspond to the case where $\lambda \gg L$ so that electrons will easily be lost to the walls before having a collision. Nevertheless, within the lower range of pressures/Knudsen numbers we investigate here, stochastic heating is usually argued as being the dominant heating component, and hardwall models used to quantitatively describe it [3–5, 16]. Thus this represents a valid range of values to study in order to answer the question posed in the title and introduction.

4. Results

4.1. Test-particle simulations

Because we are particularly interested in understanding whether electron heating can occur in the imposed electric field profiles obtained from the full PIC simulations, for these tests we load electrons with an initial Maxwellian velocity distribution having a low temperature of $T_e = 1$ eV. The TP simulations (with collisions turned on or off) are then run until equilibrium, which typically requires about 1000–2000 rf periods. Once equilibrium is reached, the electron energy probability function (EEPFs), density, current density, and power absorption (found from $P_{\text{abs}} = EJ_e$) are calculated and averaged over a number of rf periods.

Figure 4 shows a comparison of the EEPFs obtained from the TP simulations with those from the full PIC at 100 mTorr for the narrow-gap simulations. As seen, with collisions off, the final distribution function is quite close to the initial Maxwellian distribution, and no hot tail or bi-Maxwellian distribution is seen. The apparent depletion of electrons with energies above about 12 eV demonstrates that once these high-energy electrons escape the discharge, collisionless heating alone is not able to repopulate the distribution. This is in strong contrast to the EEPF obtained when collisions are turned on, which is very different from the initial distribution, and shows strong evidence of a hot tail, which agrees with the EEPF from the full PIC simulations and experiment [2]. This distribution function agrees better with experiment than the full PIC, because the electric field (which has been averaged at the correct phase over a number of rf periods) used greatly reduces the noise level in the TP simulations (see appendix A for further discussion), which are known to play a role in numerically distorting the EEPF [6]. For the wide-gap simulations (not shown), evidence of a hot tail is however observed in some of the lowest pressures simulations when collisions are turned off. The results in figure 4 however show that a bi-Maxwellian distribution can be produced as a result of collisional interactions alone, presumably because low-energy electrons cannot access the heating regions near the sheath due to reflection by ambipolar potentials in the plasma.

Figure 5 shows a comparison of the power absorption in the TP and full PIC. With collisions on the power absorption profile is very similar in shape to that from the full PIC, whereas with collisions off there is a marked difference. In addition to sharp positive and wide negative absorption peaks near the sheath, there are no power losses near the boundaries; in stark contrast with the results when collisions are turned on and the full PIC. This indicates that few particles escape the discharge when collisions are off, as is confirmed by measuring the electron current density at the walls (not shown) which is typically one or two orders of magnitude below that when collisions are on for the narrow-gap simulations, or five times smaller for the wide-gap simulations. There is also a slight asymmetry in the power absorption when collisions are turned off. Because

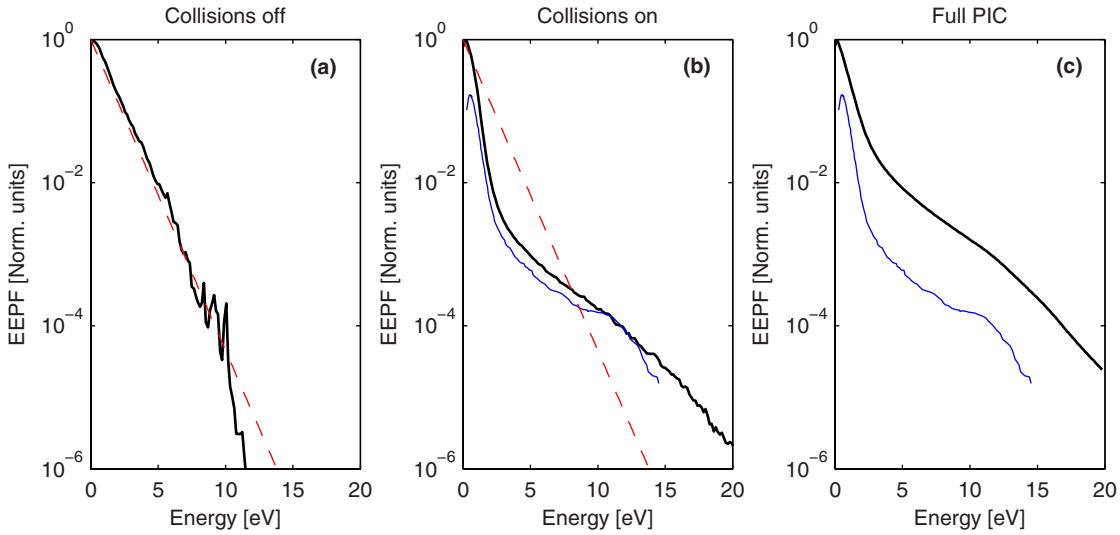

Figure 4. Simulated EEPFs for (a)–(b) the TP simulations and (c) from the full PIC simulation. The gap length is 2 cm, the pressure is 100 mTorr, and the rf current density amplitude is 25.6 Am^{-2}. The dashed lines show the EEPF of the initial Maxwellian distribution loaded into the TP simulations, while the thin lines in (b)–(c) show experimental results taken from [2].

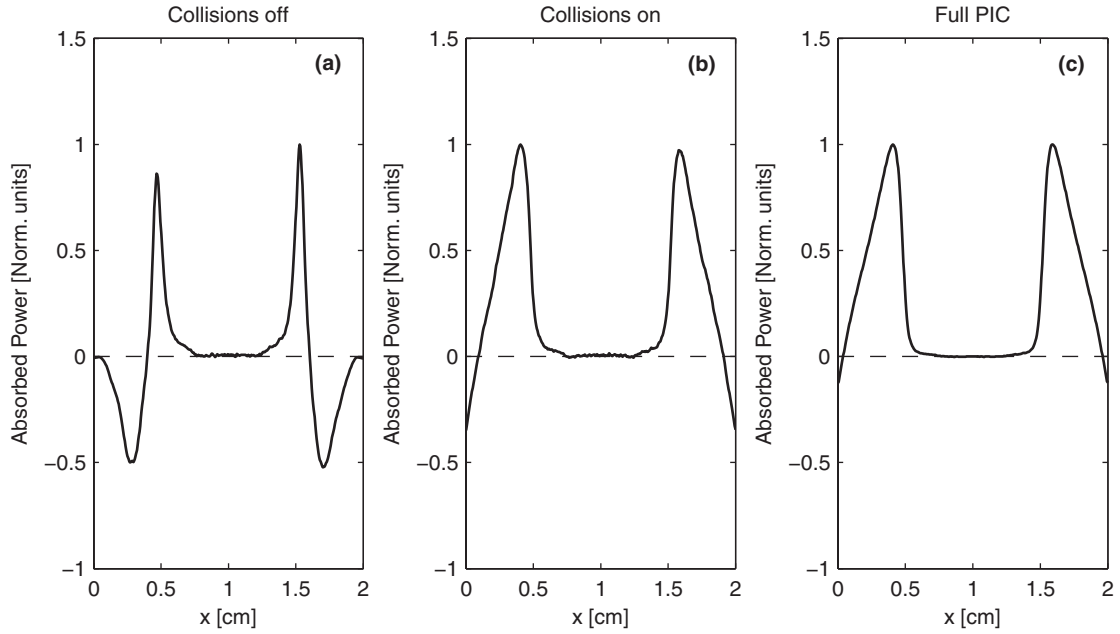

Figure 5. Time-averaged spatial profiles of the electron power absorption for (a)–(b) the TP simulations and (c) from the full PIC simulation. The gap length is 2 cm, the pressure is 100 mTorr, and the rf current density amplitude is 25.6 Am^{-2}.

of the lack of any randomization mechanisms in these simulations, any asymmetry in the initial loaded distribution and/or initial phase of the applied rf fields, can become difficult to symmetrize.

The results in figures 4 and 5 suggest that the level of true collisionless/stochastic electron heating is likely to be very low. Although the pressure of 100 mTorr used with collisions on is relatively high, this corresponds to conditions where collionless/stochastic heating is usually used to explain the non-ohmic electron heating contribution [2, 16]. We can confirm the results above by explicitly estimating the ratios of the true collisionless, $1-\eta$, and collisional, η, power absorption to the total power absorption, where

$$\eta = \frac{P_{\mathrm{C}} - P_{\mathrm{NC}}}{P_{\mathrm{C}}} = 1 - \frac{P_{\mathrm{NC}}}{P_{\mathrm{C}}} \tag{4}$$

Here P_{NC} is the total power with collisions off, and P_{C} is the total power with collisions on. We highlight that this latter term includes both ohmic heating, and any non-local/collisionless heating that is present, while P_{NC} includes only the true collisionless heating. Consequently the difference $P_{\mathrm{C}} - P_{\mathrm{NC}}$ is viewed as the total collisional (local and/or non-local) heating. These relative heating ratios are shown in figure 6 for both the narrow and wide-gap simulations. The vertical dashed lines approximately indicate the lowest pressure where a discharge can be sustained experimentally [2, 7] and using the

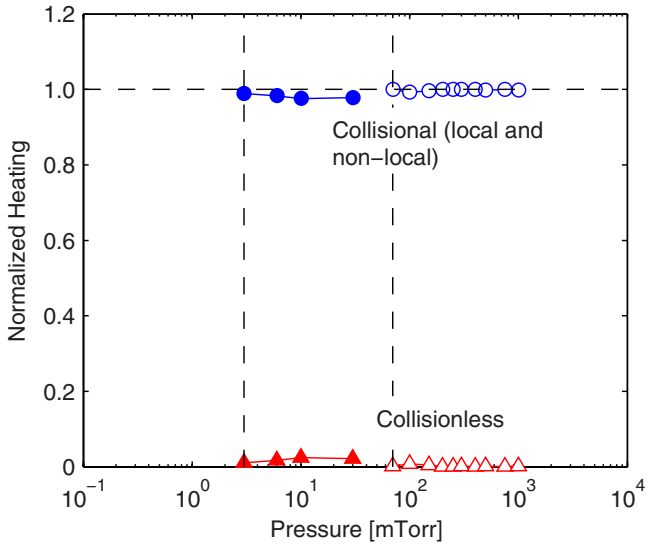

Figure 6. Ratios of the collisional power absorption (circles; this includes both local and any possible non-local contributions) and the true collisionless power absorption (triangles) to the total power absorption. The open markers correspond to a gap length of 2 cm and an rf current density amplitude of 25.6 Am^{-2}, while the closed markers correspond to a gap length of 6.7 cm and an rf current density amplitude of 10 Am^{-2}. The vertical dashed lines denote the approximate lower pressure threshold for sustaining a plasma in the narrow and wide-gap discharges respectively.

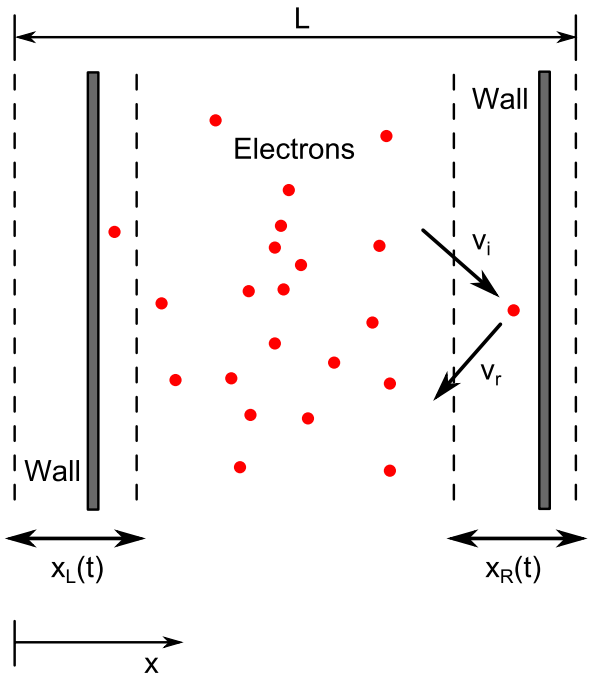

Figure 7. Schematic of the toy model simulation. The left-hand side and right-hand side walls oscillate with a position given by equation (5), while any particles that strike these walls are perfectly reflected (in the frame of reference of the wall). There is no electric field located between the walls, but a uniform neutral gas is present to allow for the possibility of collisions.

full PIC. Even with the wide-gap simulations at the lowest pressures where $\lambda \sim L$, we see that the level of true collisionless/stochastic heating is essentially negligible. Therefore in answer to the question posed in the introduction, it appears that 'collisionless/stochastic' heating in fact requires heavy particle collisions, thus confirming the predictions of non-local kinetic theory from [26].

The above results were obtained by using test particles taken from an initial non-drifting Maxwellian distribution with a temperature of 1 eV. If however a different distribution is used, such as that obtained from the full PIC simulations (see section 2), the results are found to remain similar, suggesting that the above conclusions are not sensitive to the initial distribution function chosen.

4.2. Toy model

The concept of non-local collisional heating can be more easily demonstrated by making use of a simple pedagogical toy model simulation. In this simulation we track the trajectories of electrons which interact with two oscillating boundaries, as illustrated in figure 7. The boundaries are viewed as the rf sheath edges of a CCP, and whose position changes in time according to the rf sheath model proposed by Lieberman [3, 18]. Although more accurate sheath models have been developed [33, 34], for simplicity and to maintain consistency with previous hardwall theoretical models [18, 21], we continue to use the model by Lieberman. In this model, the position, x_R, of the right-hand side boundary (for example) is given by

$$\frac{x_R}{s_0} = (1-\cos\theta) + \frac{H}{8}\left(\frac{3}{2}\sin\theta + \frac{11}{18}\sin 3\theta - 3\theta\cos\theta - \frac{1}{3}\theta\cos 3\theta\right) \tag{5}$$

where $s_0 = u_{\mathrm{wall}}/\omega$, $\theta = \omega t$, and ω is the angular frequency of the discharge. The position of the left-hand side boundary, x_L, oscillates in a similar manner, but with a phase shift of π. While the variables u_{wall} and H can be expressed in terms of other plasma parameters (see [3, 18]), we view them here simply as parameters which affect the shape and amplitude of the oscillation profile of the boundaries. Electrons which collide with either boundary are perfectly reflected (in the reference frame of the boundary), and hence model collisions with an rf sheath in a similar manner to that used in the hardwall model [3]. Thus colliding particles gain energy when the boundaries are moving inwards, and lose energy when the boundaries are moving outwards. A uniform neutral gas is located between the boundaries, and collisions (using the same Monte Carlo Collision algorithm from the full PIC and TP simulations) can be turned on or off. Poisson's equation however is not solved, and there is no electric field between the boundaries. As a result, ohmic heating does not exist, and any power absorption observed must either be truly collisionless/stochastic, or due to non-local collisional interactions.

If the boundaries are stationary and collisions are turned off, then the average electron energy remains constant with time. By then allowing the boundaries to oscillate and performing different tests with collisions turned on or off, the average electron energy can be observed with time. Simulations have been run with values of H between 0–20, u_{wall} between $1\times10^3 - 1\times10^5$ ms^{-1}, and discharge lengths

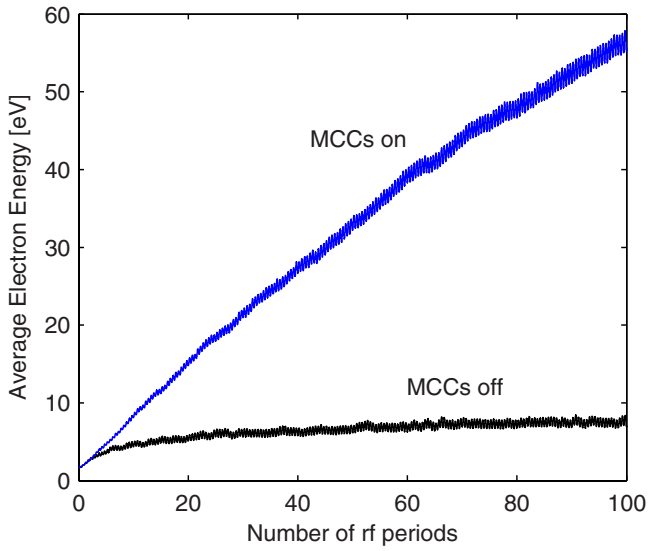

Figure 8. Average electron energy as a function of time in the toy model simulations with collisions off, and elastic collisions on (at a pressure of 3 mTorr). The gap length is 6.7 cm, $H = 6$, and $u_{\text{wall}} = 5 \times 10^4\ \text{ms}^{-1}$.

between 1–10 cm. In almost all cases the simulation behaviour is similar: with collisions turned off the electron distribution initially changes and the average electron energy increases in time until saturating after a few hundred rf periods. By contrast, with elastic collisions turned on, no definite equilibrium state is reached, and the electron energy increases unbounded. Since there are no power losses in this case (inelastic energy losses are turned off), and since ohmic heating does not exist, this indicates the presence of non-local collisional heating; an energy gain occurs when collisions happen at a different location to where the electron reflection from the sheath happens. Figure 8 shows the average electron energy with time for a typical simulation.

If inelastic energy losses are now activated, then the electron energy no longer increases unbounded, but saturates after a few hundred rf cycles. However, since continual energy losses are occurring due to ionization (we do not add new particles into the simulation, we just model the energy loss) and excitation, continual electron heating is occurring, even though there is no electric field, and no ohmic power deposition. As an example, figure 9 shows both ν/Ω, and the electron power absorption, as a function of gas pressure for $H = 6$ and $u_{\text{wall}} = 5 \times 10^4\ \text{ms}^{-1}$. Here we have used 10 000 electrons and a representative macroparticle weight of 5×10^9. Also shown is the power absorption when collisions are turned off. In this case the power absorption is not exactly zero, but is nevertheless very low. As seen, for very low pressures similar to those used in experiments and the TP simulations, significant heating can occur which is orders of magnitude larger than the true collisionless heating. Even for much lower pressures where $\lambda \gg L$, the power absorption with collisions on is significantly larger than with collisions off. This again confirms the theoretical results in [26], and in addition we note that the scaling of the absorbed power in figure 9 is consistent with those results: i.e. for $\nu/\Omega > 1$ (region B in figure 2) collisions

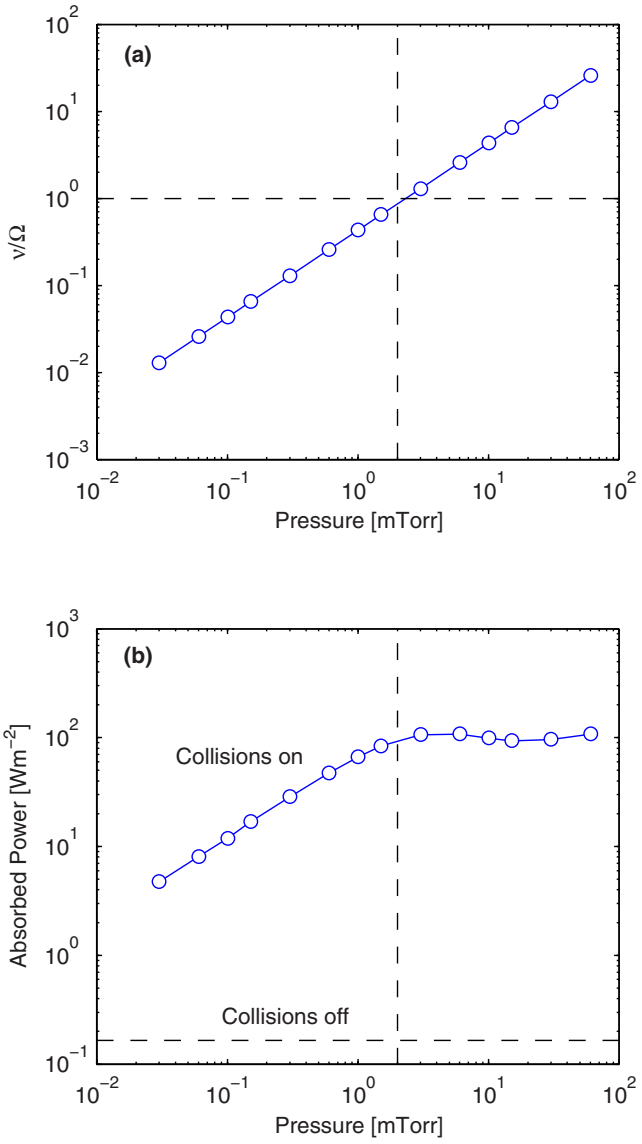

Figure 9. (a) Ratio of the collision frequency to the bounce frequency, ν/Ω, and (b) absorbed power in the toy model simulations as a function of neutral gas pressure. The gap length is 6.7 cm, $H = 6$, and $u_{\text{wall}} = 5 \times 10^4\ \text{ms}^{-1}$. With collisions on, both elastic and inelastic collisions are present (no new particles are added for ionization reactions however). The horizontal dashed line in (b) shows the level of heating observed with collisions off, while the vertical dashed lines in (a)–(b) denote the pressure where $\nu/\Omega = 1$.

are needed for heating but the absorbed power is independent of the pressure (and hence collision frequency), while for $\nu/\Omega < 1$ and $\omega/\Omega < v/\Delta v$ (region C) the absorbed power is almost linear with pressure.

4.3. Reconciliation with theoretical collisionless heating models

We have shown in the sections above that collisions are important for electron heating, even at very low pressures, and that the level of stochastic heating in bounded CCPs appears to be very small. However, if this is true, why then do collisionless

Fermi-acceleration/hardwall models seem to agree well with PIC simulations as in [16, 25]?

In this regard we can identify two separate types of PIC simulations used: a semi-infinite code [25], and a bounded code [16]. In the semi-infinite code electron-neutral collisions are not treated, and electrons are injected with a given distribution and oscillating current density at one boundary, while the opposite boundary is grounded and perfectly absorbing. Because of the injected electron current, an rf sheath forms near the grounded wall. These PIC simulations however are not self-consistent; particles of a given distribution are injected at one boundary, and any particles that are heated at the oscillating sheath at the opposite boundary are removed from the discharge when they again cross the first boundary. Thus there is an artificial break in the phase coherence between the electron motion and the sheath electric fields, and so the simulations of [25] do not truly predict collisionless/stochastic heating.

In the bounded code of [16], a full PIC simulation is used that treats both boundaries, as well as electron-neutral collisions. Here the collisionless heating is not directly calculated in the simulations, but rather is inferred by estimating the ohmic heating contribution, and subtracting this from the total electron power absorption. For these simulations pressures between 10–30 mTorr were used with a gap length of 5 cm, and an rf excitation frequency of 27.12 MHz. Tests were also performed with a lower pressure of 3 mTorr and a larger gap length of 11 cm. Based on the electron heating classification scheme discussed in section 3, this corresponds to $3 < \nu/\Omega < 10$ for the 5 cm gap length, and ν/Ω of about 2 for the 11 cm gap length. Thus these cases have a normalized parameter range that falls within those tested in sections 4.1 (see also figure 3), and which corresponds to the hybrid heating regime where true collisionless/stochastic heating is not expected to be dominant (as was confirmed in section 4.2).

Reference [16] nevertheless obtained good agreement with the hardwall model of Kaganovich *et al* [21]. As discussed in section 1 though, the hardwall model only treats a semi-infinite plasma, and does not self-consistently determine the electron distribution function. Thus again there is an artificial break in the phase coherence between the electron motion and the oscillating sheath edge that is not addressed or discussed in these theoretical models. Hence true collisionless/stochastic heating is not actually predicted. This non-local break in phase coherence does however play a similar role to electron-neutral collisions, and thus we argue here that hardwall models do not predict true collisionless/stochastic heating, but rather non-local collisional (or hybrid) heating. The good agreement obtained in [16] then indicates that this hybrid heating is relatively well described by the model of Kaganovich *et al* [21]. The fact that the crude 'phase randomization' present in these theoretical heating models seems to work reasonably well is possibly related to the results of section 4.2 (specifically figure 9); for $\nu/\Omega > 1$, although collisions are needed to produce a net heating in this regime, the absorbed power is independent of the pressure/collision frequency itself.

5. Conclusions

We have investigated electron heating over a range of different operating conditions typically encountered in many CCP reactors, and have found that true collisionless/stochastic heating contributes only a small amount to the total power absorption. These results confirm the predictions made in [26], and show that in fact collisions are needed to generate the non-ohmic heating component which has usually been attributed to collisionless/stochastic heating. Although the results of section 4.1 (and in particular, figure 6) suggest that this contribution is less than a few percent, a definitive quantitative comparison is difficult to establish. This is because in general the electron distribution function changes when collisions are turned on or off in the TP simulations, yet the absorbed power is expected to depend to some extent on the details of this distribution. Nevertheless the results show that collisionless heating cannot be the dominant power deposition mechanism and that for the small values of ν/Ω tested, non-local collisional effects are significantly more important. The importance of this non-local collisional heating has also been demonstrated using a simple phenomenological toy model in which ohmic heating is formally absent. Our results have been reconciled with recent theoretical and simulation studies by arguing that the standard hardwall model approach is not self-consistent, and that the artificial break in particle-field phase coherence that occurs mimics the effect of heavy particle collisions.

The simulations presented here have been analysed within the framework of the electron heating classification scheme introduced in [26] which is based on the non-local formulation of kinetic theory [28] and the concept of the energy diffusion coefficient. While these theories have been validated in atomic gases [35, 36], CCPs are complex systems, especially when multiple frequencies and/or molecular gases are used. Thus we cannot claim that collisionless/stochastic heating is unimportant in all conceivable CCP discharges. Nevertheless, our results show that rather than being viewed as a certainty in low pressure plasmas, true collisionless heating should rather be viewed as an exception.

By validating the predictions of [26], we can ask if there are any heating regimes where true collisionless/stochastic heating is expected to dominate. This regime corresponds to region E in figure 2. However, because this regime requires both $\omega/\Omega > \nu/\Delta\nu$, as well as $\lambda \gg L$ (see equation (2)) to access, and because it is difficult to experimentally and numerically sustain a plasma in this range, such a regime is not commonly encountered in practice. Thus again electron heating is primarily a collisional phenomenon, and we therefore argue that the terms 'collisionless heating' or 'stochastic heating' as usually used, are misleading and might be better replaced with another term, such as non-local collisional heating, or hybrid heating (to be consistent with [26]).

Acknowledgments

The authors would like to thank I Kaganovich, V Godyak, J Schulze, M Turner, A Lichtenberg, and Z Donko for a number

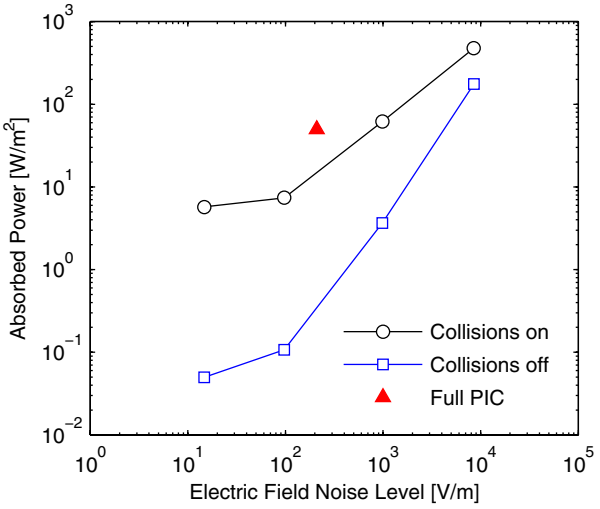

Figure A1. Absorbed power in the TP simulations as a function of the artificially added noise level. The potential profiles used are from full PIC simulations at 100 mTorr, a gap length of 2 cm, and a current density amplitude of 25.6 Am^{-2}. The closed triangle shows the absorbed power from the full PIC.

of useful comments and discussions. This work received financial state aid managed by the Agence Nationale de la Recherche as part of the program 'blanc' under the reference ANR-2011-BS09-40 (EPIC), and the program 'Investissements d'avenir' under the reference ANR-11- IDEX-0004-02 (Plas@Par).

Appendix A. The effect of statistical noise

Because of the statistical nature of PIC simulations, it is well known that the level of numerical noise depends on the number of particles used. Particularly for CCP simulations using argon (which has a Ramsauer minimum in the elastic scattering cross-section), it has been found that a large number of particles are required in order to prevent numerical heating of the low energy electron population [6, 37]. In order to reduce noise levels in the TP simulations we have used plasma potential profiles from PIC simulations that have been averaged over many hundreds of rf periods (at the correct rf phase). Thus the electric field profile is significantly smoother than that typically seen by the particles in full PIC simulations. The TP simulations however offer a useful approach to more explicitly investigate the effect of numerical noise. To demonstrate this we consider a number of example simulations where we add Gaussian noise to the electric field profiles. Since the noise in PIC simulations is usually strongest in the bulk plasma where the electric field is smallest, we spatially modulate the noise level by using the normalized electron density profile:

$$E(x,t) = E(x,t) + E_0\, h(x) R(x,t) \qquad \text{(A.1)}$$

where E is the electric field, E_0 is a noise amplitude level, $h(x)$ is the normalized electron density profile (obtained from the full PIC simulations), and $R(x,t)$ is a normally distributed random number (with a mean of zero, and a standard deviation of one) chosen at each spatial position, x, and at each time, t.

Figure A1 shows the electron power absorption at different noise levels when collisions are turned on (at a pressure of 100 mTorr) and off. The closed triangle shows the heating obtained from the full PIC, where the noise level is estimated as the 1-σ level of the unaveraged electric field in the bulk plasma with respect to a strongly filtered/smoothed field. With the noise amplitude, E_0, set to zero in equation (A.1), the residual noise level is similar to the noise level of the left most point in figure A1. At low noise levels, the true collisionless heating is more than a hundred times smaller than that present when collisions are turned on. As the noise level increases, both the collisionless and collisional heating increases. In particular, at noise levels similar to full PIC simulations, the collisionless heating has increased by an order of magnitude. These results echo well known concerns previously raised [38] about using PIC simulations instead of Vlasov codes to model collisionless phenomena, since the numerical noise level in PIC codes can be as much as 10^4 times higher than Vlasov simulations. The noise can therefore be viewed as playing a somewhat similar role to that of particle collisions, and consequently introduces an artificial phase randomization/stochastization even if particle collisions are removed. Eventually at sufficiently high noise levels, the effect of particle collisions becomes less and less important, as the grid induced 'collisions' begin to dominate. The difference between the absorbed power from the full PIC (closed triangle) and the TP simulations with collisions on (open circles) at similar noise levels, is most likely due to the fact that in the full PIC the numerical noise is not truely random, but is correlated with the motion of the PIC particles.

References

[1] Popov O A and Godyak V A 1985 *J. Appl. Phys.* **57** 53
[2] Godyak V A and Piejak R B 1990 *Phys. Rev. Lett.* **65** 996
[3] Lieberman M A and Lichtenberg A J 2005 *Principles of Plasma Discharges and Materials Processing* (New York: Wiley)
[4] Chabert P and Braithwaite N 2011 *Physics of Radio-Frequency Plasmas* (Cambridge: Cambridge University Press)
[5] Turner M M 2009 *J. Phys. D: Appl. Phys.* **42** 194008
[6] Vahedi V, Birdsall C K, Lieberman M A, DiPeso G and Rognlien T D 1993 *Plasma Sources Sci. Technol.* **2** 273
[7] Godyak V A, Piejak R B and Alexandrovich B M 1992 *Plasma Sources Sci. Technol.* **1** 36
[8] O'Connell D, Gans T, Vender D, Czarnetzki U and Boswell R 2007 *Phys. Plasmas* **14** 034505
[9] Mahony C M O and Graham W G 1999 *IEEE Trans. Plasma Sci.* **27** 72
[10] Schulze J, Heil B G, Luggenhölscher D, Mussenbrock T, Brinkmann R P and Czarnetzki U 2008 *J. Phys. D: Appl. Phys.* **41** 042003
[11] Vender D and Boswell R W 1990 *IEEE Trans. Plasma Sci.* **18** 725
[12] Wood B P 1991 Sheath heating in low pressure capacitive radio frequency discharges *PhD Dissertation* University of California, Berkeley
[13] Surendra M and Graves D B 1991 *IEEE Trans. Plasma Sci.* **19** 144
[14] Surendra M and Dalvie M 1993 *Phys. Rev.* E **48** 3914
[15] Lafleur T, Chabert P and Booth J P 2014 *Plasma Sources Sci. Technol.* **23** 035010

[16] Kawamura E, Lieberman M A and Lichtenberg A J 2014 *Phys. Plasmas* **21** 123505
[17] Godyak V A 1972 *Sov. Phys. Tech. Phys.* **16** 1073
[18] Lieberman M A 1988 *IEEE Trans. Plasma Sci.* **16** 638
[19] Turner M M 1995 *Phys. Rev. Lett.* **75** 1312
[20] Gozadinos G, Turner M M and Vender D 2001 *Phys. Rev. Lett.* **87** 135004
[21] Kaganovich I D, Polmarov O V and Theodosiou C E 2006 *IEEE Trans. Plasma Sci.* **34** 696
[22] Lafleur T, Chabert P, Turner M M and Booth J P *Plasma Sources Sci. Technol.* **23** 015016
[23] Kawamura E, Lieberman M A and Lichtenberg A J 2006 *Phys. Plasmas* **13** 053506
[24] Schulze J, Donkó Z, Derzsi A, Korolov I and Schuengel E 2015 *Plasma Sources Sci. Technol.* **24** 015019
[25] Sharma S and Turner M M 2013 *Plasma Sources Sci. Technol.* **22** 035014
[26] Kaganovich I D, Kolobov V I and Tsendin L D 1996 *Appl. Phys. Lett.* **69** 3818
[27] Kaganovich I D and Tsendin L D 1992 *IEEE Trans. Plasma Sci.* **20** 86
[28] Tsendin L D 1995 *Plasma Sources Sci. Technol.* **4** 200
[29] Birdsall C K and Langdon A B 1985 *Plasma Physics Via Computer Simulation* (New York: McGraw-Hill)
[30] Turner M M, Derzsi A, Donkó Z, Eremin D, Kelly S J, Lafleur T and Mussenbrock T 2013 *Phys. Plasmas* **20** 013507
[31] Heil B G, Brinkmann R P and Czarnetzki U 2009 *J. Phys. D: Appl. Phys.* **42** 085205
[32] Phelps A V and Petrović Z Lj 1999 *Plasma Sources Sci. Technol.* **8** R21
[33] Godyak V A and Sternberg N 1990 *Phys. Rev.* A **42** 2299
[34] Czarnetzki U 2013 *Phys. Rev.* E **88** 063101
[35] Busch C and Krotshagen U 1995 *Phys. Rev.* E **51** 280
[36] Kortshagen U, Pukropski I and Tsendin L D 1995 *Phys. Rev.* E **51** 6063
[37] Kim H C, Manuilenko O and Lee J K 2005 *Jpn. J. Appl. Phys.* **44** 1957
[38] Kolobov V I and Arslanbekov R R 2006 *IEEE Trans. Plasma Sci.* **34** 895